Latex Interpenetrating Polymer Networks Based on Acrylic Polymers. III. Synthesis Variations

D. J. HOURSTON,* R. SATGURUNATHAN,† and H. VARMA,
Department of Chemistry, University of Lancaster, Bailrigg, Lancaster, LA1 4YA, United Kingdom

Synopsis

Two latex interpenetrating polymer networks, one from a supposedly compatible pair and the other from an incompatible pair of polymers, were prepared by two-stage emulsion polymerization. The synthesis conditions in each case were varied by altering the ratio of the glassy polymer to the rubbery polymer and also by reversing the order of synthesis. Fabricated samples of these latex interpenetrating polymer networks were subjected to hardness, stress-strain, and dynamic mechanical measurements. Hardness and stress-strain measurements showed that, although the second formed polymer dominated the final mechanical properties, the compatibilities of the polymer pairs played an important role. Dynamic mechanical analysis for the inverse systems showed evidence of enhanced mixing.

INTRODUCTION

Latex interpenetrating polymer networks (LIPN) are a unique type of polymer blend prepared by two-stage emulsion polymerization methods.[1-3] LIPNs have been claimed by many workers to exhibit complex morphologies including the core-shell and cellular structures. Important variables in terms of controlling IPN morphology[4-7] include the relative amounts of the two polymers, the order of synthesis, the crosslink density of each network, the miscibility of the second monomer in the first formed polymer network, the hydrophilicity of the polymers involved, and the level of compatibility of the selected pair of polymers.

In a previous paper in this series,[8] we discussed 1:1 LIPNs based on polyethyl acrylate and polyethyl methacrylate (PEA/PEMA), denoted as system E, and on polyethyl acrylate and poly-*t*-butyl acrylate (PEA/PtBA) denoted as system F. Using transmission electron microscopy (TEM) and dynamic mechanical analysis (DMA), an essentially core-shell model for these latex particles was proposed. To substantiate further the existence of this morphology, further studies were carried out on the above systems by altering some of the synthetic conditions employed in the polymerization. The variations employed in this study fall into three main categories. (i) Altering the

*To whom correspondence should be addressed.
†Present address: School of Chemistry, University of Bristol, Bristol, England BS8 1TS.

Journal of Applied Polymer Science, Vol. 33, 215–225 (1987)
 CCC 0021-8995/87/010215-11$04.00

composition of polymer 2. (ii) Inverting the order of synthesis. (iii) Investigating the effect of the time of swelling of polymer 1 in monomer 2. The first two of these variations are the subject of this paper. The influence of swelling time will be the topic of a later paper.

The combination of different types of polymeric networks covering a range of compositions has resulted in controlled morphologies and has been shown[4,6] to produce IPNs with certain synergistic behavior. If one polymer is a glass and the other is elastomeric, a reinforced rubber is obtained when the elastomeric component is predominant. A high-impact plastic is obtained if the glassy component is continuous and predominant. In this study, the glassy component, PEMA in system E and PtBA in system F, was varied to 1 : 2 and 1 : 3 ratio with respect to the rubbery component, PEA. The properties of these materials were compared with those of the corresponding 1 : 1 composition.

Inverting the order of synthesis in LIPNs has been shown to alter the transition behavior and thus mechanical properties.[3] In particular, the second formed polymer network tends to exhibit a stronger glass transition than expected from the overall composition, and the seed latex network yields a correspondingly weaker transition. To study these effects inverse IPNs of systems E and F, namely PEMA/PEA (E′) and PtBA/PEA (F′), were prepared. The same synthetic procedure as for the normal systems was employed, except of course, for the order of monomer addition. Thus, in E′ and F′, polymer 1 is the glassy component and polymer 2 the rubbery component.

TABLE I
Hardness Numbers of LIPNs and of the Homopolymer Networks

Sample	Shore (type D) hardness numbers
Homopolymer	
PEA	—
PEMA	78
PtBA	71
LIPN System	
System E	
PEA/PEMA	
1 : 1	55
1 : 2	66
1 : 3	69
Inverse E′	
PEMA/PEA	
1 : 1	52
System F	
PEA/PtBA	
1 : 1	49
1 : 2	61
1 : 3	65
Inverse F′	
PtBA/PEA	
1 : 1	41

Experimental

The LIPNs were prepared using the two-stage emulsion polymerization method described previously.[9] Hot pressed samples of the coagulated latex were obtained for mechanical measurements.

The hardness of the LIPNs, together with those of the respective homopolymer networks, were assessed by static indentation tests using a Shore type D durometer.

The stress-strain measurements were made using a J. J. Lloyd tensometer, model T 5002. All tensile measurements were conducted on dumb-bell-shaped samples at 20°C and at a strain rate of 10 mm/min. A Polymer Laboratories Dynamic Mechanical Thermal Analyser was used for the dynamic mechanical analysis. The heating rate was maintained at 2°C/min throughout all the runs and an impressed frequency of 10 Hz was employed.

RESULTS AND DISCUSSION

Hardness Measurements

Hardness of polymeric materials is generally defined as the resistance to local deformation. It is essentially a surface property, but is related to

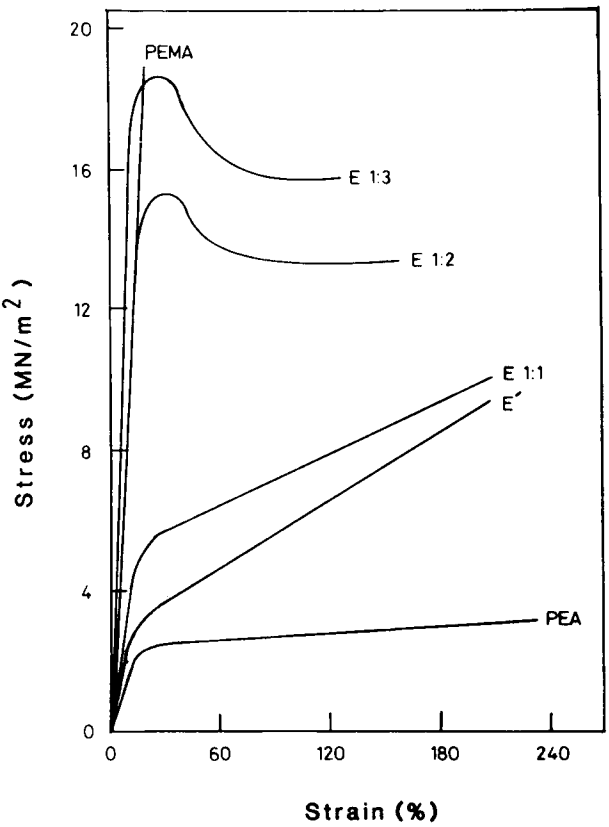

Fig. 1. Stress-strain curves for system E: (i) with increasing glassy polymer content, (ii) the inverse system E′, and (iii) the respective homopolymer networks.

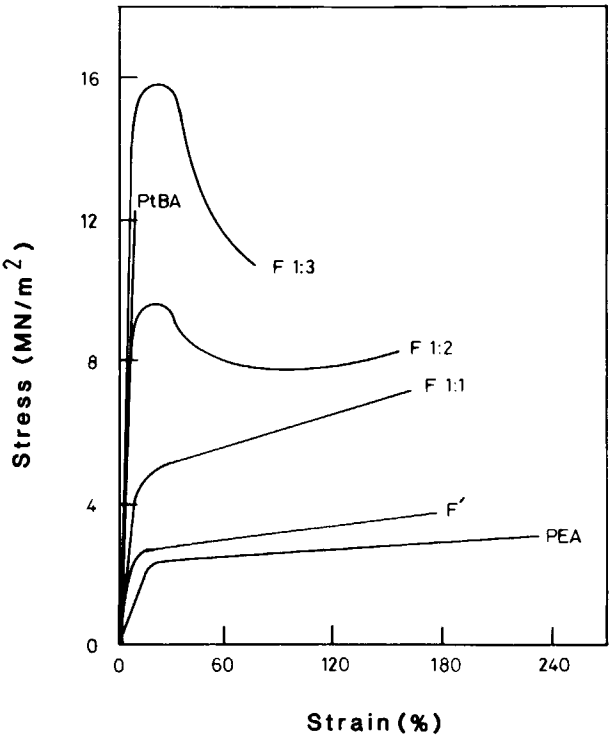

Fig. 2. Stress-strain curves for system F: (i) with increasing glassy polymer content, (ii) the inverse system F′, and (iii) the respective homopolymer networks.

TABLE II
Stress-Strain Properties of the LIPNs and Homopolymer Networks at 20°C

Sample	Initial modulus (MN/m^2)	Stress at break (MN/m^2)	Strain at break (%)
Homopolymer			
PEA	66.4	3.2	233
PEMA	442.6	18.4	—
PtBA	359.0	12.1	—
LIPN System			
System E			
PEA/PEMA			
1 : 1	76.0	10.1	211
1 : 2	114.0	13.6	160
1 : 3	150.0	15.8	129
Inverse E′			
PEMA/PEA			
1 : 1	60.8	9.3	204
System F			
PEA/PtBA			
1 : 1	88.8	7.3	169
1 : 2	156.0	8.5	157
1 : 3	269.0	10.8	75
Inverse F′			
PtBA/PEA			
1 : 1	34.4	3.7	168

mechanical properties such as modulus, strength and elasticity.[10,11] The results (Table I) are expressed as an average of four measurements. From Table I, it is evident that, as the composition of polymer 2 is increased, a significant increase in hardness occurs for both systems E and F.

For the inverse systems, E′ and F′, where the rubbery component, PEA, is polymer 2, a significant lowering in hardness might be expected relative to the corresponding normal systems. However, it is seen that only F′ exhibits a really significant lowering in hardness. This lowering in the hardness of F′ could possibly be attributed to the relatively strong incompatibility[9] of PEA and PtBA which could result in a more definite core-shell morphology. The relatively insignificant lowering in the hardness of E′ may indicate that there is some mixing of the two networks, and, consequently, a less distinct core-shell particle morphology results. This interpretation is consistent with earlier[9] results.

Stress-Strain Measurements

Figures 1 and 2 show the stress-strain curves of systems E and F together with their respective homopolymer networks. Also shown in the same figures are the stress-strain curves for the inverse systems E′ and F′. The essential details from these curves are summarized in Table II.

In the case of the 1:1 LIPN system E, the initial modulus is seen to decrease to a value close to that of the PEA homopolymer. However, upon increasing the amount of the glassy polymer the initial modulus increases. This increase, although not very large, does imply that the glassy polymer component is becoming increasingly more continuous. The increase in the stress at break value, together with the decrease in the elongation at break complement this interpretation.

In the case of system F, when the amount of PtBA is increased, the initial modulus also increases as in system E, but does so to a much greater extent. This implies that the PtBA network is more continuous in F than is the PEMA network in system E. As explained earlier,[9] this is believed to be the

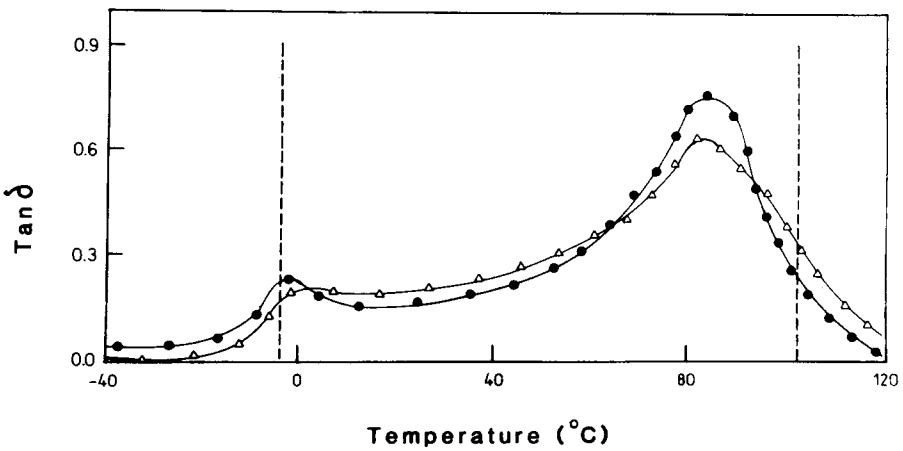

Fig. 3. Tan δ-temperature curves for normal LIPN system E (●) and the inverse system E′ (Δ) at 10 Hz. The broken lines indicate the peak positions of the corresponding homopolymer networks.

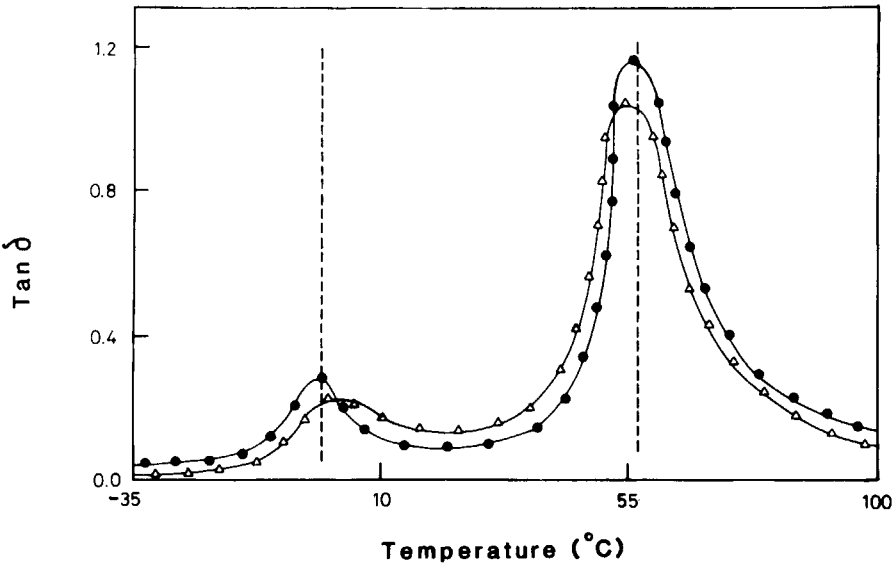

Fig. 4. Tan δ-temperature curves for normal LIPN system F (●) and the inverse system F′ (Δ) at 10 Hz. The broken lines indicate the peak positions of the corresponding homopolymer networks.

result of the greater inherent incompatibility of the PEA/PtBA system, which results in a more distinct core-shell particle morphology.

In the case of the inverse systems, E′ and F′, it is seen that the initial modulus and stress at break values for the inverse systems are lower than those of their respective normal systems, indicating that PEA is now the more continuous phase. However, it is interesting to note that the magnitude of the lowering in the initial modulus and the stress at break values for system F′ is quite large in comparison with those for system E′. The large decrease in the system F′ values is most likely the result of the marked incompatibility of PEA and PtBA, leading to a well defined core-shell morphology, which results in the pressed sheets having the rubbery component as the more continuous

TABLE III
Glass Transition Temperatures of the LIPNs and the Corresponding Homopolymer Networks at 10 Hz (° C)

Polymer	Network 1	Network 2
PEA	−4	—
PEMA	—	104
PtBA	—	58
System E		
PEA/PEMA	−2	84
Inverse E′		
PEMA/PEA	0	82
System F		
PEA/PtBA	−4	58
Inverse F′		
PtBA/PEA	−2	55

TABLE IV
Tan δ Half-Peak Widths of the Higher Temperature Transitions of the LIPNs

LIPN	Tan δ half-peak width (°C)
E : PEA/PEMA	38
E′ : PEMA/PEA	47
F : PEA/PtBA	19
F′ : PtBA/PEA	22

TABLE V
Intertransition tan δ Values for the LIPNs

LIPN	Intertransition value
E : PEA/PEMA	0.17
E′ : PEMA/PEA	0.19
F : PEA/PtBA	0.07
F′ : PtBA/PEA	0.11

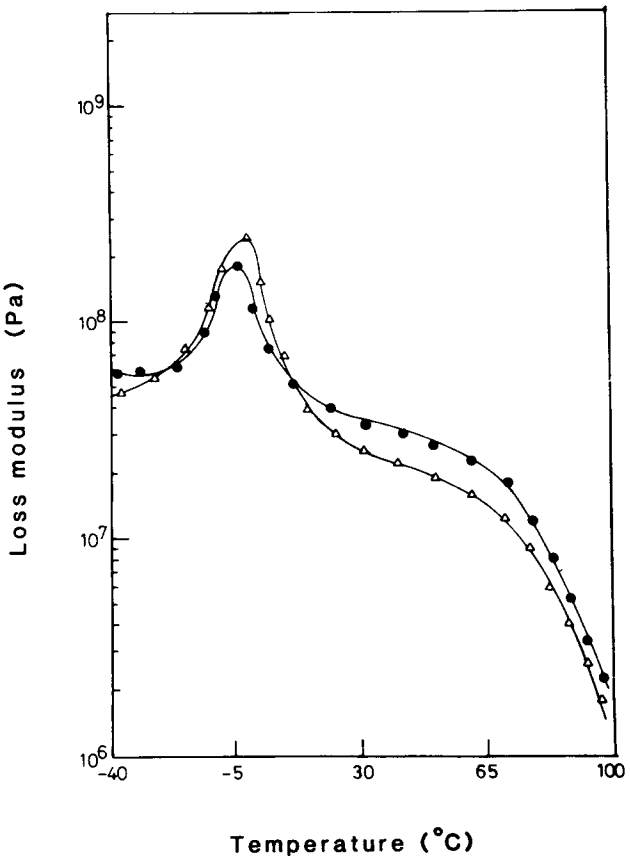

Fig. 5. Loss modulus-temperature plots for normal LIPN system E (●) and the inverse system E′ (Δ) at 10 Hz.

phase. The relatively insignificant lowering of these values for E′ arises because of the partial compatibility of PEA with PEMA. Consequently, the dominance of the second formed network is reduced as a result of the partial mixing of the two networks.

Dynamic Mechanical Analysis

The tan δ plots as a function of temperature for inverse systems E′ and F′ together the corresponding normal systems are shown in Figures 3 and 4. The glass transition temperatures (Tg) obtained from these plots are given in Table III. It is evident from these figures that the shape of the overall plots and the position of the peaks are different from those of the normal systems. In both the inverse systems the polymer 1 and the polymer 2 tan δ peaks are shifted slightly inward on the temperature scale with respect to the corresponding homopolymer networks. The inward shifting of the peaks in polymer blends has been shown by many workers to be an indication of some degree of mixing.[12] Hence, on this basis, it can be said that the levels of mixing in the inverse systems is greater than in the respective normal systems.

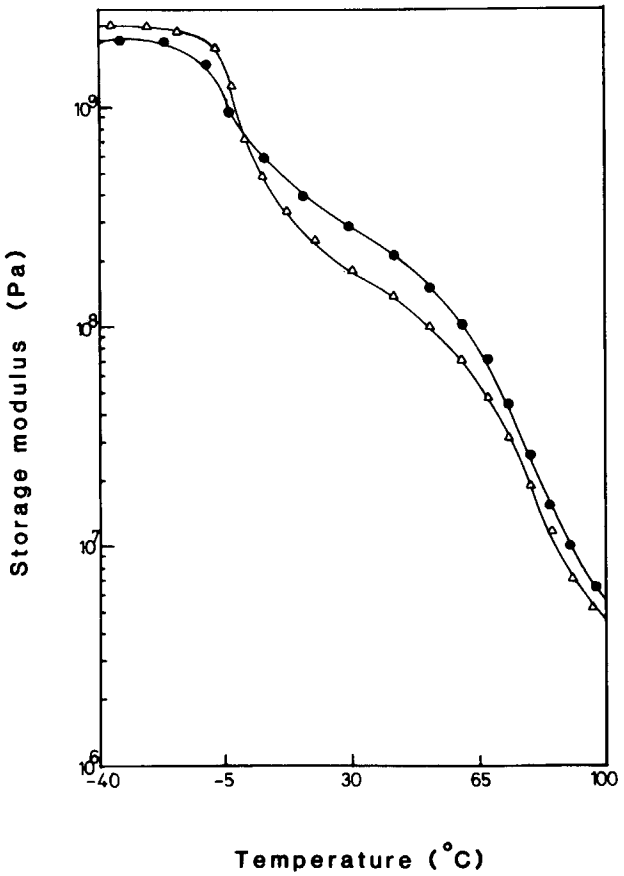

Fig. 6. Storage modulus-temperature plots for normal LIPN system E (●) and the inverse system E′ (Δ) at 10 Hz.

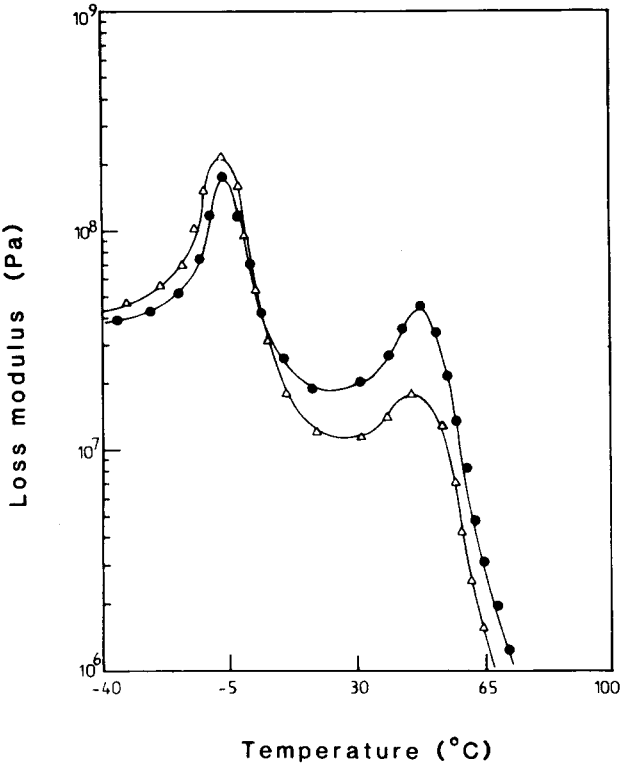

Fig. 7. Loss modulus-temperature plots for normal LIPN system F (●) and the inverse system F′ (Δ) at 10 Hz.

The shapes of the tan δ-temperature plots of the normal and inverse systems are also interesting. In the case of E′, the lower temperature network peak is much less well resolved and the second network peak is broadened. Table IV shows the tan δ half-peak widths for systems E and F. It is seen that in the case of E′ the second peak is broadened by about 9°C, suggesting enhanced mixing. In the case of F′, though not as significant as with E′, a similar broadening of the second transition is observed (3°C). This reduction would be expected for an intrinsically more incompatible system.

Further evidence for enhanced molecular mixing in the inverse systems can be obtained by looking at the intertransition value of tan δ.[8] If more mixing occurs and there is, therefore, an overlap of the relaxation time distributions of the components, these intertransition values of tan δ should be larger. Table V shows the tan δ intertransition values for both normal and inverse systems. It is seen that both inverse systems exhibit higher values, indicating that the level of mixing in the inverse systems is higher than in the normal systems. Figures 5 to 8 show the loss and storage modulus-temperature curves for inverse systems E′ and F′. Also shown on the same plots are the curves for the corresponding normal systems. Comparison of storage and loss modulus-temperature data for systems E and E′ (Figs. 5 and 6) indicates that the lower temperature transition, which arises from essentially the PEA component, is more prominent for the E′ LIPN. This would be consistent with an inverse

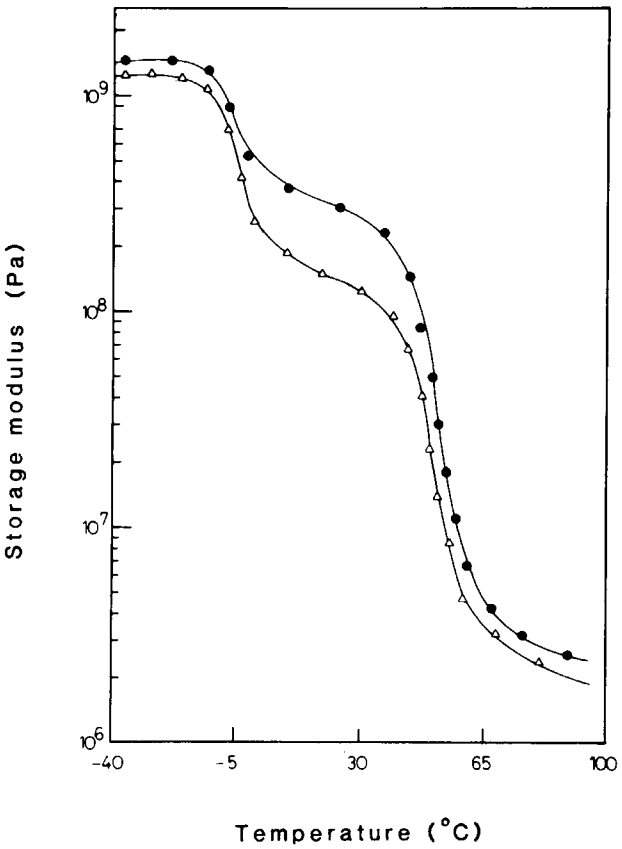

Fig. 8. Storage modulus-temperature plots for normal LIPN system F (●) and the inverse system F′ (Δ) at 10 Hz.

LIPN particle morphology in which the PEA component is present, at least substantially, on the outside of the particles. Sheet pressed from polymer consisting of particles with such a morphology would have a continuous phase with a high PEA content. Similar results were obtained for systems F and F′ (Figs. 7 and 8).

From the above results, both inverse systems show evidence for a degree of mixing of the two networks. In system E, the extent of mixing in the inverse system is greater than that in the normal system. In system F, the evidence suggests that little or no mixing is present in the normal system, but the inverse system seems to exhibit some slight degree of mixing.

References

1. L. H. Sperling, *Interpenetrating Polymer Networks and Related Materials*, Plenum, New York, 1981.

2. L. H. Sperling, T. W. Chiu, R. G. Gramlich, and D. A. Thomas, *J. Paint Technol.*, **46**, 47 (1974).

3. L. H. Sperling, T. W. Chiu, and D. A. Thomas, *J. Appl. Polym. Sci.* **17**, 2443 (1973).

4. P. Keusch and D. J. Williams, *J. Polym. Sci. Polym. Chem.*, **11**, 143 (1973).

5. P. Keusch, J. Prince, and D. J. Williams, *J. Macromol. Sci. Chem.*, **3**, 623 (1973).
6. S. Muroi, H. Hashimoto, and K. Hoshi, *J. Polym. Sci. Polym. Chem.*, **22**, 1365 (1984).
7. D. I. Lee and T. Ishikawa, *J. Polym. Sci. Polym. Chem.*, **21**, 147 (1983).
8. D. J. Hourston and R. Satgurunathan, *J. Appl. Polym. Sci.*, **31**, 1955 (1986).
9. D. J. Hourston and R. Satgurunathan, *J. Appl. Polym. Sci.*, **29**, 2969 (1984).
10. D. Kerry, J. A. Brydson, and K. J. Saunders, *Rubber and Plastic Testing*, Chapman and Hall, London, 1963.
11. P. I. Donnelly, *Encyclopedia of Polymer Science and Technology*, Vol. 7, Wiley, New York, 1967.
12. L. H. Sperling, D. W. Taylor, M. L. Kirkpatrick, H. F. George, and D. R. Bradman, *J. Appl. Polym. Sci.*, **14**, 73 (1970).

Received May 13, 1986
Accepted July 1, 1986